

Section II. Applications in medicine, biology, low-energy and X-ray physics

BONE DENSITOMETRY WITH A HIGH-SPEED, HIGH-RESOLUTION MWPC

F. ANGELINI, R. BELLAZZINI, A. BREZ, M.M. MASSAI and M.R. TORQUATI

Dipartimento di Fisica dell'Università di Pisa and INFN Sezione di Pisa, Via Livornese 582/A, S. Piero a Grado, I-56010 Pisa, Italy

A method for the assessment of bone mineral content of the peripheral skeleton is presented. The method makes use of a multiwire proportional chamber (MWPC) as a photon counting and imaging area device. The system can work as a single-photon absorptiometer (SPA) at the energies of both ^{125}I and ^{153}Gd . It can also work as a dual-photon absorptiometer (DPA) using one of the two pairs of isotopes ^{125}I , ^{153}Gd or ^{125}I , ^{241}Am . Both the calcaneus and the forearm can be imaged in a few minutes, either with single- or dual-photon absorptiometry.

1. Introduction

The quantitative assessment of bone mineral content (BMC) and of bone mineral density (BMD) is a primary diagnostic tool. A precise determination of these parameters is a necessary index for the diagnosis of osteoporosis and other pathological conditions of the skeleton.

The methods existing for this assessment have variable precision, accuracy, sensitivity and cost. The most important ones are: (1) single-photon absorptiometry (SPA), (2) dual-photon absorptiometry (DPA), (3) quantitative computed tomography (QCT) and (4) combined cortical thickness (CCT) measurements.

What is required by the measurement methods listed above is essentially: (1) high sensitivity for early detection of small changes of bone mass (which are of the order of a few per cent per year), (2) good reproducibility over short and long periods for longitudinal studies on the same patient, (3) the capability of discriminating between cortical and trabecular bone, (4) access to different regions of the skeleton, (5) an easy and user-friendly procedure for the operator and the patient, (6) low cost and (7) low radiation exposure to the patient.

No single technique can fulfill all these requirements [1]. The main limitations of the widely available single- and dual-photon absorptiometry of the appendicular skeleton are related to the inability to measure trabecular and cortical bone separately, and to repositioning error. This source of error is connected with the difficulty of measuring the bone mineral density at the (more interesting) very distal site of the forearm. Indeed, the rate of change per unit length of bone density at the very distal site of the forearm is much steeper than at more proximal sites [2]. The aim of this work is to present a new method for the assessment of bone mineral content which, thanks to its flexibility, sensitivity and speed, should avoid or reduce these limitations

and, therefore, have several advantages over the standard SPA and DPA.

2. Materials and methods

2.1. Hardware

The system we have developed can be operated either as SPA or DPA. For both SPA and DPA we have used several radioactive sources with energy lines in the range 27–60 keV and activity in the range 50–300 mCi (see table 1). When operating the system as SPA, the first step of the measurement procedure is to take a transmission image of the forearm or of the calcaneus immersed in a water bath. The recording device is an electronic detector (MWPC) which counts and measures the X–Y coordinates of the photons transmitted through the object. The MWPC is a gas area detector commonly used for high-energy physics experiments. It is made up of a grid of uniformly spaced thin anode wires, sandwiched between two outer grids of mutually orthogonal strips of wires (cathodes). Conceptually, it may be thought of as an array of single wire proportional

Table 1
 Characteristics of radioactive sources used

SPA ^{a)}	^{153}Gd	^{125}I	–
	50 mCi	300 mCi	
	42 keV X-ray	27 keV X-ray	
DPA ^{b)}	^{153}Gd	^{125}I	^{241}Am
			100 mCi
			60 keV X-ray

^{a)} SPA = single photon absorptiometry.

^{b)} DPA = dual photon absorptiometry.

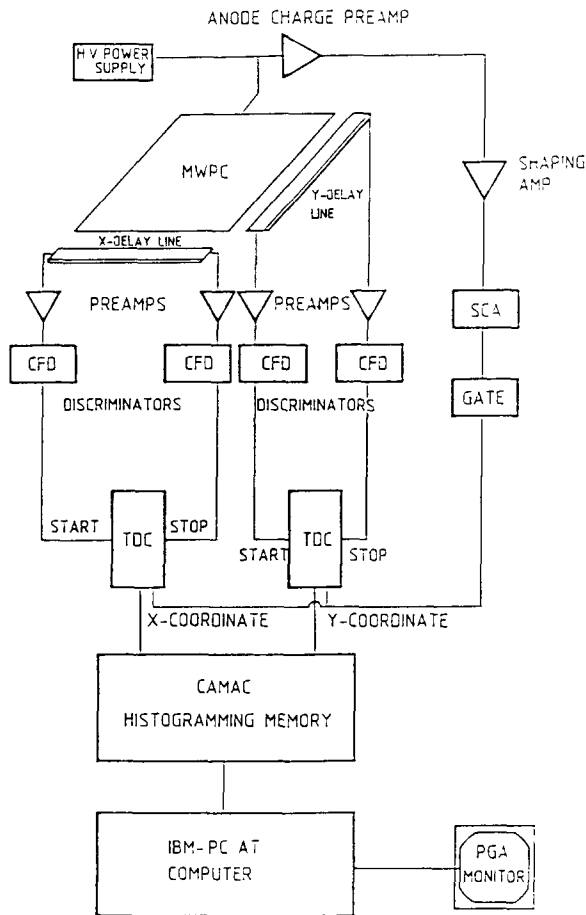


Fig. 1. A schematics of the detector and its associated electronics.

counters, placed side by side, which act independently. The electron avalanche resulting from an X-ray interaction with the atoms of the filling gas induces a signal onto two orthogonal delay lines, which are capacitively coupled to the cathode planes. Two time-to-digital converters (TDC) convert the transit time on the delay line of each axis into X and Y coordinates which are stored in a digital memory and subsequently transmitted to a personal computer (IBM PC-AT) for analysis. The charge signal deposited on the anode wire plane is proportional to the energy deposited in the chamber by the X-ray event and can be used, in combination with a single-channel analyzer (SCA), for pulse height analysis. A gray or color real-time image of the X-ray transmission pattern through the object is displayed by means of an image processing system (IBM-PGA), consisting of a matrix of 640×480 pixels, each 8 bits deep. Fig. 1 shows the schematics of the detector and its associated electronics, while fig. 2 shows an overall view of the system. A more detailed description of the whole apparatus is reported elsewhere [3]. The unique characteristics of the detection system for the present application may be summarized as follows: (1) it is xenon-filled and pressurized up to 3 atm to increase the detection efficiency ($\approx 15\%$ at 42 keV), (2) the active area is $128 \times 128 \text{ mm}^2$ and the spatial resolution is 1 mm for both coordinates and (3) it can operate at high data rate (up to 200 kHz). When operating the system as a SPA, a second image (reference image) of the water bolus is taken to subtract the contribution of the soft tissue.

The technique of DPA allows one to avoid the use of the water bolus, thus simplifying the procedure and giving access to more regions of the human skeleton.

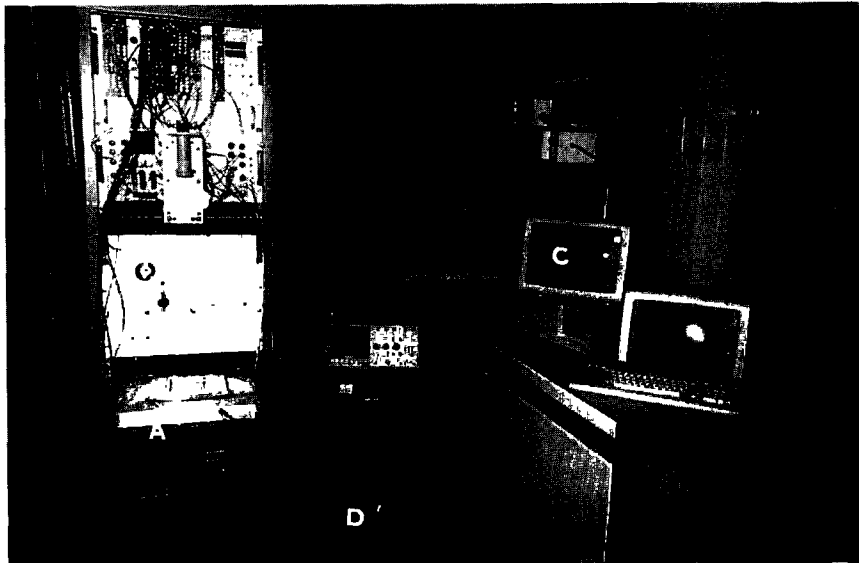


Fig. 2. An overall view of the system: (A) MWPC, (B) signal processing electronics, (C) data acquisition system, (D) water bolus.

The contribution of the soft tissue is cancelled by taking two images at two different energies and logarithmically subtracting the low-contrast image (reference image) from the high-contrast image (transmission image), after having weighted the former with the ratio of the attenuation coefficients of muscle at the two energies. A detailed description of DPA theory is reported in ref. [4]. For MWPC-DPA we have utilized two pairs of isotopes, ^{125}I , ^{153}Gd and ^{125}I , ^{241}Am . While the first pair is optimized in terms of detection efficiency (because of the low energy lines of both the isotopes) the second pair is optimized in terms of the contrast of the final image (because of the large difference of the attenuation coefficients of bone at 27 and 60 keV).

As with all area detectors, the MWPC can suffer from the problem of the detection of scattered radiation. This problem can be particularly severe for SPA, because of the large scatter fraction due to the water bolus. To reduce this fraction to a few percent, two orthogonal antiscatter grids (manufactured by GILARDONI-Lecco-Italy) with a cell depth/width ratio of 12 were placed in front of the chamber entrance window.

In the present version, for both MWPC-SPA and MWPC-DPA, the data acquisition speed is ≈ 40 kHz. This speed is not set by the readout electronics (which has an upper limit of ≈ 200 kHz), but rather by the source activity. Exploiting the full rate capability of the device will shorten the acquisition time to a few tens of a second.

2.2. Software

After having recorded the transmission and the reference images in SPA or DPA mode, a software program performs a logarithmic subtraction of the reference picture from the transmission picture. The content of each pixel of the new image (densitogram) is proportional to the bone mass at that point. This picture can be thought of as being made of hundreds of profiles such as those obtained with standard SPA or DPA and placed side by side. Figs. 3a and 3b show the SPA transmission image and the densitogram of the forearm obtained with the MWPC after subtraction of the soft tissue contribution. These pictures were obtained in 4 min using the 42 keV line. Figs. 3c and 3d show the corresponding SPA images obtained at 27 keV. The use of the lower energy provides a much better image contrast, thus lowering the acquisition time (2 min in this case) and increasing the precision of the positioning procedure). These advantages are particularly evident when measuring patients with a very low BMC and BMD. Fig. 4 shows the images obtained with the patient having the lowest values of BMC and BMD in our data sample. The beneficial effect of the ^{125}I source for the positioning procedure and the area definition, is



Fig. 3. (ab) Transmission image of the forearm immersed in a water bath and the densitogram obtained with a ^{153}Gd source; (cd) The same results for (a) and (b) obtained with ^{125}I source, (ef) DPA image of the forearm obtained with the Gd, I and Am, I pairs, respectively; (g) DPA image of the calcaneus obtained with the Am, I pair.

quite evident. The disadvantages of the 27 keV energy line is the short lifetime of the source ($T_{-1/2} = 60$ days) and that its use is limited to thin regions. Figs. 3e and 3f show the DPA densitograms of the forearm obtained with the MWPC making use of the ^{153}Gd , ^{125}I sources and of the ^{241}Am , ^{125}I sources, respectively. Fig. 3g shows the DPA densitogram of the calcaneus obtained with the MWPC using the ^{241}Am , ^{125}I sources. On all these images it is quite easy to identify several position reference points (the ulnar styloid tip, the subchondral cortex, etc.) which can be used to define the measurement area. A cursor can be moved on the image to

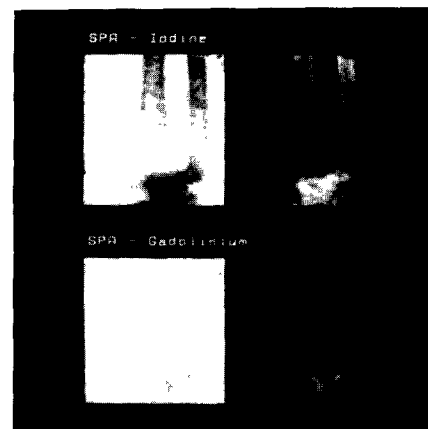


Fig. 4. An example of the beneficial effect of the use of ^{125}I when imaging patients with severe osteoporosis.



Fig. 5. An example of the operation of the program which computes the area, the BMC and the BMD of various regions of radius and ulna. On top of the image the histograms of BMD computed at each individual line are displayed.

select one or more of these reference points. The interactive nature of the analysis procedure allows one to obtain a high repositioning precision (≈ 1 mm) which is particularly important for longitudinal studies on the same patient and for investigating sites which have very different shapes like the calcaneus and the forearm. For a quantitative evaluation of MWPC-SPA of the forearm, a special piece of software was developed. First the program asks the operator for the position of the $\frac{1}{10}$ distal line (distal and proximal refer to the distance from the body axis).

Using this information and the selected position reference points, the program identifies 4 regions for both the radius and the ulna: (1) a very distal region which starts ≈ 1 cm from the ulnar styloid tip, (2) a distal region, i.e. a region centered on the $\frac{1}{10}$ distal line (≈ 2.5 cm from the ulnar styloid tip), (3) a proximal region, contiguous to the distal region, and (4) a more proximal region ($\approx \frac{1}{3}$ distal). All the 4 regions span the same longitudinal length. The very distal and the distal regions partially overlap. An automatic algorithm based on a polynomial fitting procedure identifies (see fig. 5) the borders of radius and ulna with high precision (1% mean error on the determination of radius area). Having defined the area of the 8 regions (4 for radius and 4 for ulna), the program computes the mean BMC and BMD for each of them. The area BMC and BMD

computed in this way are the averages over the specified area of the line BMC and BMD computed at each individual line. The line BMC and BMD measured with the MWPC have the same meaning and are expressed with the same units of the two quantities computed by standard DPA at, for example, the $\frac{1}{10}$ distal line.

The program also determines the repositioning error, that is the new value which was obtained assuming a preset error (1 or more pixels) of the positioning procedure. Finally the histograms of the BMC and BMD obtained at each line are plotted as a function of the

Table 2
Axial rate of change of BMC and BMD in radius (values are in %/mm)^{a)}

Site	$\frac{\{d(\text{BMC})/dx\}}{\text{BMC}}$		$\frac{\{d(\text{BMD})/dx\}}{\text{BMD}}$	
	line	area	line	area
Distal	1.6	0.8	2.6	1.7
$\frac{1}{10}$ dist.	1.0	0.5	1.6	1.0
Med. prox.	0.7	0.3	1.0	0.8
Proximal	0.7	0.3	0.9	0.6

^{a)} Table 3 reports relative rate of change of line BMC and BMD (columns 1, 3) and of area BMC and BMD (columns 2, 4)

axial displacement from the distal end of both radius and ulna. From the best fit to these histograms the axial rate of change of line BMC and BMD is evaluated at 4 points: the most distal point, the $\frac{1}{10}$ distal point the proximal point and the most proximal point. The repositioning error depends on the absolute value of this rate of change, i.e. the higher the speed of change, the larger will be the effect of, for example, 1 mm repositioning error. These derivatives can be used for estimating the sensitivity of standard DPA to the repositioning error. Table 2 reports the axial rate of change of area BMC and BMD and of line BMC and BMD as measured with the MWPC in SPA mode in a group of 76 patients. The rate of change of area BMC is half of that of line BMC, while the rate of change of area BMD is $\frac{2}{3}$ of that of the corresponding line BMD.

Several times a day an SPA densitogram of a 5 mm thick reference block of aluminum was taken to monitor the stability and reproducibility of the procedure. The percentage standard deviation of these calibration measurements was $\approx 1\%$.

3. Discussion

It is widely accepted that any measurement technique having access to regions rich in trabecular bone has an evident advantage relative to techniques that can access only the less responsive cortical bone [1]. MWPC absorptiometry can access the calcaneus and, because of its very low repositioning error, the very distal site of the forearm. The calcaneus is a weight-bearing, fully trabecular bone and for this reason it should have a biological behaviour similar to that of spinal trabecular bone. The very distal site of the forearm is the richest of trabecular bone, with a relative abundance similar to that of the vertebral bodies [2]. The measurement of the bone mineral content at the calcaneus and at the very distal end of the forearm is therefore a fairly good index for diagnosis of osteoporosis and the assessment of the risk of vertebral fractures as it has been shown in a recent longitudinal and perspective study on more than one thousand patients by Wasnich and coworkers [5]. Furthermore MWPC absorptiometry has a higher sensitivity than the standard DPA or SPA of the forearm because it measures BMC and BMD over an extended area, thus lowering the statistical and positioning error. From the final image it is also possible to extract several other parameters, like the axial change of BMC and BMD, which could find useful applications.

From a more general point of view, MWPC absorptiometry is characterized by low cost (of the same order of magnitude of standard SPA) and by low dose (less than $10 \mu\text{Gy}$). The examination is quite easy to perform. However, the MWPC has some limitations in the present implementation: (1) it is not useable for

Table 3
Monte Carlo detection efficiency [%] versus photon energy (E) and gas pressure (P)

E [keV]	P [atm]			
	1	2	3	4
40	18.8	29.4	35.1	37.8
50	10.9	18.3	23.2	26.3
60	6.8	11.7	15.3	18.0
70	4.7	8.2	10.9	12.9
80	3.1	5.5	7.4	8.9
90	2.2	4.0	5.4	6.5
100	1.7	3.0	4.1	5.0

regions other than extremities, and (2) it is not possible to discriminate anatomically between the cortical and trabecular components of the bone. We think it will be possible to remove the first limitation with a different design of the system. To study this problem in detail we have developed a Monte Carlo program simulating several detector configurations. This program models to process of absorption of the impinging radiation (40–100 keV) with the filling gas (Xe, CO_2), the subsequent random clustering ionization, the drift movement of electrons toward the anode wires and the distribution of the collected charge on the anode plane. It is therefore possible to optimize the design of the detector in terms of gap thickness, pressure, gas filling, energy of the incoming radiation, etc. Table 3 shows an example of the results obtained for the detection efficiency at various energies and pressures when simulating a detector having a total thickness of 26 mm. Events corresponding to the reabsorption of the fluorescent X-ray of xenon inside the detector volume were discarded.

Table 4 shows the corresponding spatial resolution expected at the border of the detector ($128 \text{ mm} \times 128 \text{ mm}$) when a point source is placed at a distance of 1 m from the detector window. Figs. 6 and 7 show an example of the point spread-function obtained in the middle and at the border of the detector for a 70 keV source energy. Parallax, diffusion and range of pho-

Table 4
Width [mm] of simulated point spread function versus photon energy (E) and gas pressure (P)

E [keV]	P (atm)			
	1	2	3	4
40	0.45	0.45	0.44	0.44
50	0.47	0.46	0.45	0.45
60	0.56	0.48	0.47	0.46
70	0.75	0.54	0.50	0.48
80	1.03	0.64	0.55	0.51
90	1.39	0.80	0.62	0.56
100	1.80	0.99	0.74	0.63

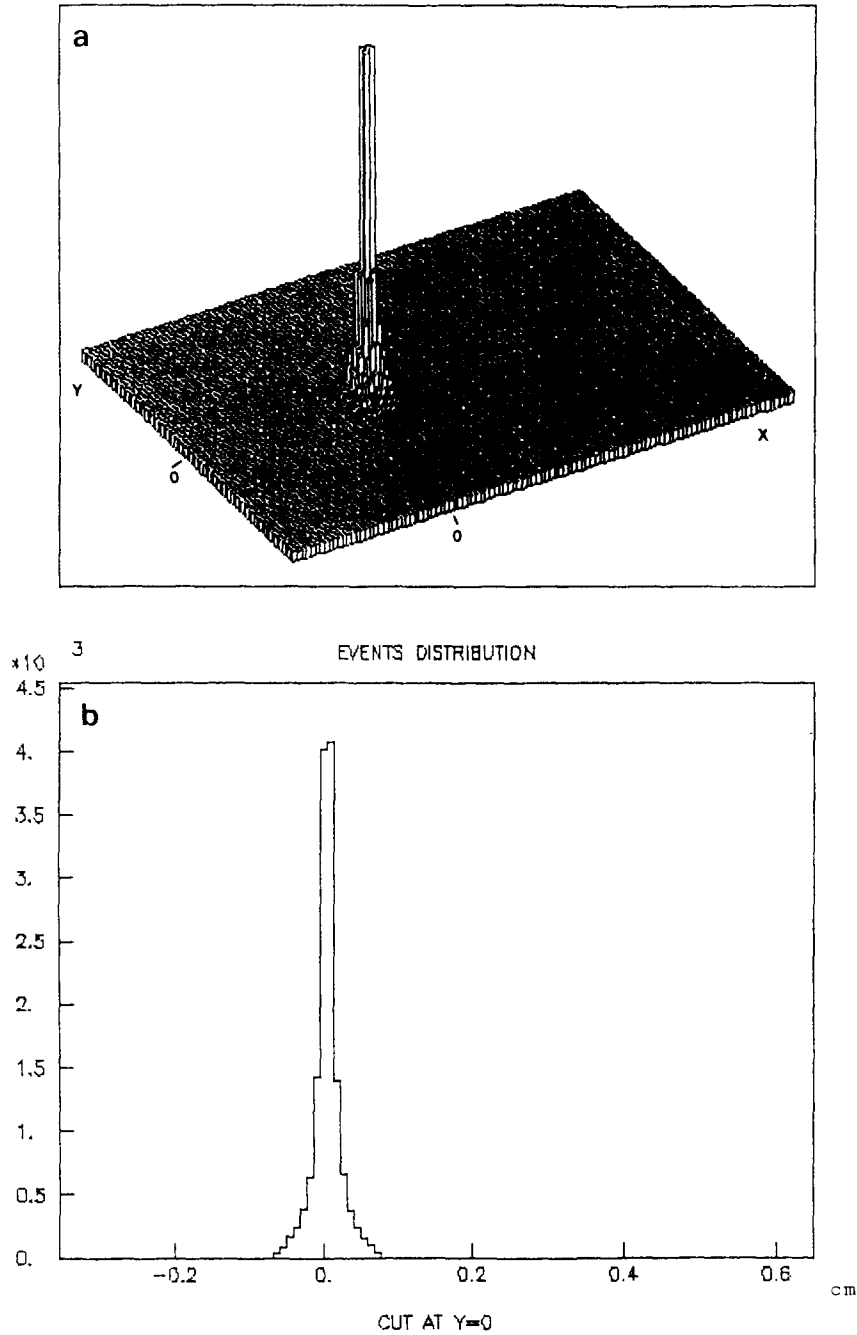
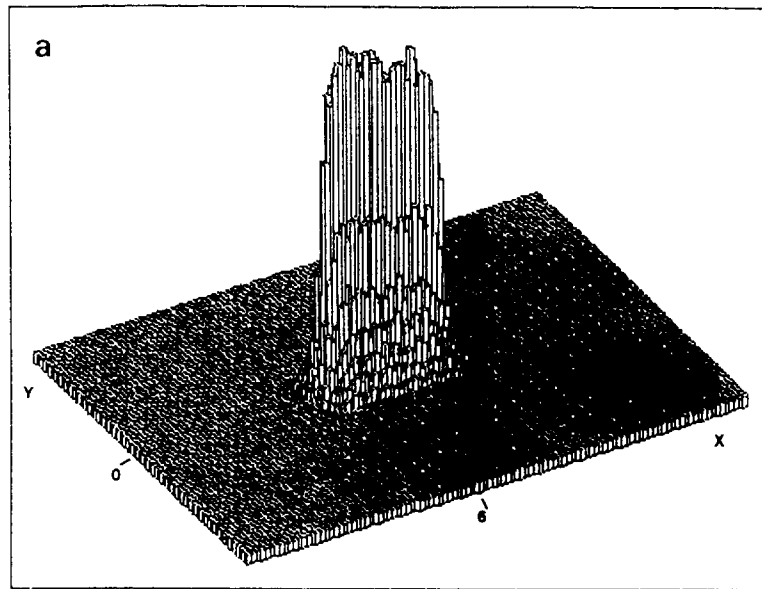


Fig. 6. (a) Scatter plot of the reconstructed events coming from a 70 keV point source placed at 1 m and impinging in the middle of the detector; (b) a cut through the center of the distribution in (a).

toelectrons were taken into account. We are now designing a new detector based on these results and which will be suitable for DPA of the lumbar spine and of the extremities. This detector will work at 40 and 70 keV with an efficiency between 10% and 35%, a spatial

resolution better than 1 mm and will make use of a high-intensity fluorescent X-ray source.

For the second limitation we emphasize that MWPC absorptiometry can measure a trabecular bone (the calcaneus), the cortical bone (at the proximal site of



EVENTS DISTRIBUTION

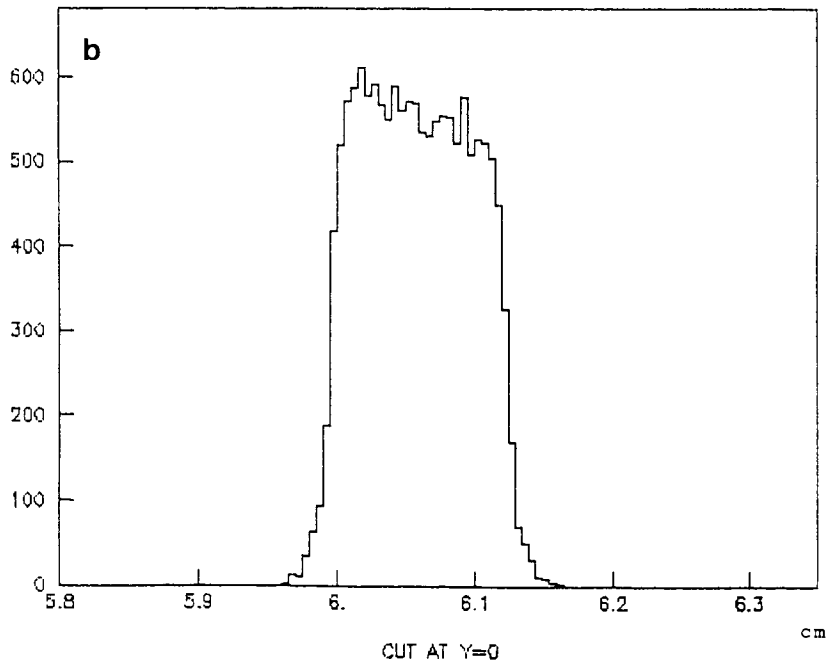


Fig. 7. The same as fig. 6 but with the source impinging on the border of the detector.

the forearm) and a mixture of cortical and trabecular bone (at the very distal site), by means of two consecutive measurements taking no more than 10 min. It should therefore be possible to estimate the rate of a trabecular bone loss in a weight-bearing bone and the individual rate of trabecular and cortical bone loss in a

non weight-bearing bone, if the bone composition at each site of the forearm is known [2].

There are also a few open questions that we will address in the future: (1) the relative advantage of using ^{125}I or ^{153}Gd sources, (2) the relative advantage of exploiting the dual energy capability for extremities

studies, and (3) the comparison of this technique with computerized tomography (CT) and DPA densitometry of the lumbar spine.

References

- [1] W. Reinbold, H.K. Genant, U.J. Reiser, S.T. Harris and B. Ettinger, *Radiology* 160 (1986) 469.
- [2] L. Nilas, H. Norgaard, J. Podenphant, A. Gotfredsen and C. Christiansen, *Scand. J. Clin. Lab. Invest.* 47 (1987) 41.
- [3] R. Bellazzini, A. Brez, A. Del Guerra, M.M. Massai and M.R. Torquati, *Nucl. Instr. and Meth.* 23 (1985) 480.
- [4] B. Roos and H. Skoldorn, *Acta Radiol. Ther. Phys. Biol.* 13 (1974) 266.
- [5] R.D. Wasnich, P.D. Ross, L.K. Heilborun and J.M. Vogel, *Am. J. Obstet. Gynecol.* 153 (1985) 745.